



## Determination of the Avogadro Constant by Counting the Atoms in a $^{28}\text{Si}$ Crystal

B. Andreas,<sup>1</sup> Y. Azuma,<sup>2</sup> G. Bartl,<sup>1</sup> P. Becker,<sup>1</sup> H. Bettin,<sup>1</sup> M. Borys,<sup>1</sup> I. Busch,<sup>1</sup> M. Gray,<sup>3</sup> P. Fuchs,<sup>4</sup> K. Fujii,<sup>2</sup> H. Fujimoto,<sup>2</sup> E. Kessler,<sup>5</sup> M. Krumrey,<sup>1</sup> U. Kuetgens,<sup>1</sup> N. Kuramoto,<sup>2</sup> G. Mana,<sup>6</sup> P. Manson,<sup>3</sup> E. Massa,<sup>6</sup> S. Mizushima,<sup>2</sup> A. Nicolaus,<sup>1</sup> A. Picard,<sup>7</sup> A. Pramann,<sup>1</sup> O. Rienitz,<sup>1</sup> D. Schiel,<sup>1</sup> S. Valkiers,<sup>8</sup> and A. Waseda<sup>2</sup>

<sup>1</sup>PTB—Physikalisch-Technische Bundesanstalt, Bundesallee 100, 38116 Braunschweig, Germany

<sup>2</sup>NMIJ—National Metrology Institute of Japan, 1-1-1 Umezono, Tsukuba, Ibaraki 305-8563, Japan

<sup>3</sup>NMI—National Measurement Institute, Bradfield Road, Lindfield, NSW 2070, Australia

<sup>4</sup>METAS—Bundesamt fuer Metrologie, Lindenweg 50, 3003 Bern-Wabern, Switzerland

<sup>5</sup>NIST—National Institute of Standards and Technology, 100 Bureau Drive, Gaithersburg, Maryland 20899, USA

<sup>6</sup>INRIM—Istituto Nazionale di Ricerca Metrologica, strada delle cacce 91, 10135 Torino, Italy

<sup>7</sup>BIPM—Bureau International des Poids et Mesures, Pavillon de Breteuil, 92312 Sèvres Cedex, France

<sup>8</sup>IRMM—Institute for Reference Materials and Measurements, Retieseweg 111, B-2440 Geel, Belgium

(Received 12 October 2010; revised manuscript received 9 December 2010; published 18 January 2011)

The Avogadro constant links the atomic and the macroscopic properties of matter. Since the molar Planck constant is well known via the measurement of the Rydberg constant, it is also closely related to the Planck constant. In addition, its accurate determination is of paramount importance for a definition of the kilogram in terms of a fundamental constant. We describe a new approach for its determination by counting the atoms in 1 kg single-crystal spheres, which are highly enriched with the  $^{28}\text{Si}$  isotope. It enabled isotope dilution mass spectroscopy to determine the molar mass of the silicon crystal with unprecedented accuracy. The value obtained,  $N_A = 6.022\,140\,78(18) \times 10^{23} \text{ mol}^{-1}$ , is the most accurate input datum for a new definition of the kilogram.

DOI: 10.1103/PhysRevLett.106.030801

PACS numbers: 06.20.Jr, 06.30.Dr, 82.80.Ms

Accurate measurements of fundamental constants are a way of testing the limits of our knowledge and technologies. In these tests, the measurement of the Avogadro constant,  $N_A$ , holds a prominent position because it connects microphysics and macrophysics. In addition, as a new definition of the kilogram most likely will be based on the Planck constant [1],  $h$ , a determination of  $N_A$  is a way to obtain an independent  $h$  value via the molar Planck constant,  $N_A h$ .

While the uncertainty of the mass of the international kilogram prototype is zero by convention, any new realization will fix an uncertainty to the kilogram; it has been agreed that the relative uncertainty of any new realization must not exceed  $2 \times 10^{-8}$ . Two experiments have the potential to achieve this goal. One is the watt-balance experiment. It aims at measuring  $h$  by the virtual comparison of mechanical and electrical powers [2]. The other experiment aims at determining  $N_A$  by counting the atoms in 1 kg nearly perfect single-crystal silicon spheres [3]. In this method, crystallization acts as a “low noise amplifier” making the lattice parameter accessible to macroscopic measurements, thus avoiding the single atom counting. Silicon is used because it is one of the best known materials and it can be grown into high-purity, large, and almost perfect single crystals.

Since 1998 [4], a relative  $1.2 \times 10^{-6}$  discrepancy has been observed when comparing the results of these experiments through  $N_A h$ . It was conjectured that it originated through the difficulty of accurately determining the

isotopic composition of a natural Si crystal, a key measurement for  $N_A$  determination. To solve this problem, we repeated the measurement by using a silicon crystal highly enriched with the  $^{28}\text{Si}$  isotope. In this way, the absolute calibration of the mass spectrometer with the required small uncertainty could be overcome by applying isotope dilution mass spectrometry combined with multicollector inductively coupled plasma mass spectrometry.

The project started in 2004 with the isotope enrichment by centrifugation of  $\text{SiF}_4$  gas undertaken at the Central Design Bureau of Machine Building in St. Petersburg. Subsequently, after conversion of the enriched gas into  $\text{SiH}_4$ , a polycrystal was grown by chemical vapor deposition at the Institute of Chemistry of High-Purity Substances of the Russian Academy of Sciences in Nizhny-Novgorod and, in 2007, the 5 kg  $^{28}\text{Si}$  boule shown in Fig. 1 was grown by the Leibniz-Institut für Kristallzüchtung in Berlin [5].

*Principle of the measurement.*—Atoms were counted by exploiting their ordered arrangement in the crystal. Provided the crystal and the unit cell volumes are measured and the number of atoms per unit cell is known, the count requires their ratio to be calculated. Hence,  $N_A = nM/(\rho a^3)$ , where  $n = 8$  is the number of atoms per unit cell,  $M/\rho$  and  $a^3$  are the molar and unit cell volumes,  $M$  the molar mass, and  $\rho$  the density. The crystal must be free of imperfections, monoisotopic (or the isotopic composition must be determined), and chemically pure. We selected a spherical crystal-shape to trace back the volume

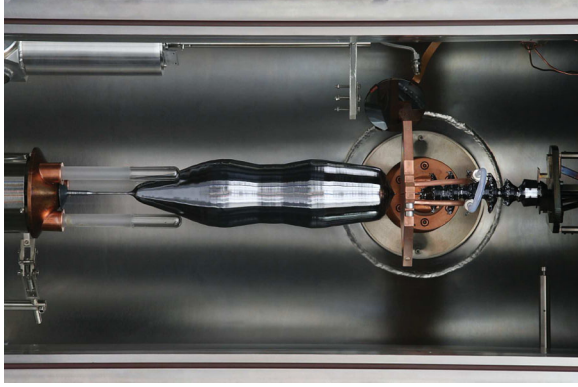


FIG. 1 (color). The float-zone  $^{28}\text{Si}$  crystal. To determine its density, two spheres were manufactured from the two bulges. To determine the lattice parameter, an x-ray interferometer was cut from the material between these spheres.

determination to diameter measurements and to make possible an accurate geometrical, chemical, and physical characterization of the surface. Hence, two spheres, AVO28-S5 and AVO28-S8, were taken at 229 mm and 367 mm distances, respectively, from the seed crystal position and shaped as quasiperfect spheres by the Australian Centre for Precision Optics.

*Imperfections.*—Our boule is dislocation free, it was purified by the float-zone technique, no doping by nitrogen was used, and the pulling speed was chosen in order to reduce the self-interstitial concentration. Unavoidable pointlike defects by carbon, oxygen, and boron atoms as well as vacancies strain the crystal and change the sphere mass. To apply the necessary corrections, their concentrations were measured by infrared spectroscopy and positron life time spectroscopy; the results are given in Table I. Laser scattering tomography excluded voids having diameters greater than the 30 nm detection limit.

*Lattice parameter.*—To measure the lattice parameter, an x-ray interferometer was fabricated from the material between the spheres. Next, the mean lattice parameter of each sphere given in Table III,  $a(S) = (1 + \sum_i \beta_i \Delta N_i) a(\text{XINT})$ , was calculated by taking account of the different contaminations of the spheres and the interferometer. In this equation,  $S$  is the sphere AVO28-S5 or -S8,  $a(\text{XINT})$  is the measured value of the interferometer lattice parameter,  $i$  labels the point defects,  $\beta_{\text{C}} = -6.9(5) \times 10^{-24} \text{ cm}^3$ ,

TABLE I. Point-defect concentration (expressed in  $10^{15} \text{ cm}^{-3}$ ) in the AVO28-S5 and AVO28-S8 spheres and in the x-ray interferometer (XINT).

Defect	AVO28-S5	AVO28-S8	XINT
Carbon	0.40(5)	1.93(19)	1.07(10)
Oxygen	0.28(6)	0.42(9)	0.37(3)
Boron	0.011(4)	0.03(2)	0.004(1)
Vacancy	0.33(10)	0.33(10)	0.33(10)

$\beta_{\text{O}} = 4.4(2) \times 10^{-24} \text{ cm}^3$ , and  $\beta_{\text{B}} = -5.6(2) \times 10^{-24} \text{ cm}^3$  are the strain coefficients [6], and  $\Delta N_i$  is the difference of the defect concentration between the spheres and the interferometer (see Table I). The lattice parameter of a number of samples, taken from both sides of the spheres, was determined via double-crystal Laue diffractometry. After corrections for the differences in the point-defect concentrations, all the measured values were found to agree within their measurement uncertainties. Lattice parameter topographies, made by using both x-ray phase-contrast imaging and a novel self-referenced x-ray diffractometer, did not show evidence of any intrinsic strain.

*Surface.*—Silicon is covered with an oxide surface layer. X-ray photoelectron spectroscopy, x-ray fluorescence, and near-edge x-ray absorption fine structure measurements on the spheres revealed unexpected surface contamination by copper and nickel-forming silicides. Therefore, to determine the surface layer mass and thickness given in Table II, the sphere surface was modeled, from top to bottom, as follows: a carbonaceous and an adsorbed water layer [7], a layer of Cu and Ni silicides, and a  $\text{SiO}_2$  layer. The oxide thickness was determined by x-ray fluorescence measurements with synchrotron radiation at BESSY II. The oxygen K fluorescence intensity from the sphere surface was compared with that from flat samples for which the oxide layer thickness was determined by x-ray reflectometry. The mass deposition of carbon, copper, and nickel was also obtained from x-ray fluorescence measurements. The stoichiometry of the oxide was determined by x-ray photoelectron spectroscopy, which also excluded the presence of a  $\text{SiO}$  interface layer. Data for chemisorbed water on silicon were taken from the literature [8]. Figure 2 shows the mapping of the surface layer thickness, obtained by spectroscopic ellipsometry with a spatial resolution of 1 mm [9].

*Mass.*—The spheres mass given in Table III was determined by comparison with the Pt-Ir prototypes of the BIPM, NMIJ, and PTB; the results are in excellent agreement and demonstrate a measurement accuracy of about  $5 \mu\text{g}$ . Corrections for the surface layers and for the crystal point defects have to be considered. Owing to point defects, there is the  $\Delta m = V \sum_i (m_{28} - m_i) N_i$  difference given in Table II between the measured mass and the mass of a perfect lattice having a Si atom on each regular site. In this equation,  $m_{28}$  and  $m_i$  are the masses of, respectively,  $^{28}\text{Si}$  and the  $i$ th point defect (a vacancy mass is zero and oxygen is associated to an interstitial lattice site, so that,  $m_{\text{O}}$  is the sum of the oxygen and the  $^{28}\text{Si}$  masses),  $V$  is the

TABLE II. Mass and thickness of the surface layer and mass deficit due to the point defects.

	Unit	AVO28-S5	AVO28-S8
Surface Layer Mass	$\mu\text{g}$	221(14)	213(14)
Surface Layer Thickness	nm	2.87(32)	2.67(31)
Mass Deficit	$\mu\text{g}$	8.1(2.4)	24.3(3.3)



FIG. 2 (color). Topographic maps of the surface layer thickness. Left AVO28-S5; right AVO28-S8. The rainbow colors range from 2.0 nm (blue) to 4.5 nm (yellow).

sphere volume, and  $N_i$  is the concentration of the  $i$ th point defect (see Table I).

*Volume.*—The sphere volumes were determined from diameter measurements carried out by optical interferometry. Two different interferometers were used, both relying on differential measurements [10]. Each sphere is placed between the end mirrors (plane, in one interferometer, spherical, in the other) of a Fizeau cavity and the distances between the mirrors and each sphere, as well as the cavity length, were measured. Since the sphere is almost perfect, its volume is that of a mathematical sphere having the same mean diameter. Hence, a number of diameters were measured and averaged. Figure 3 shows the deviations from a constant diameter in orthographic projections. The measured diameters were corrected for phase shifts in beam reflections at the sphere surface, as well for the beam retardation through the surface layer. The final volumes are given in Table III.

*Molar mass.*—The molar mass measurement requires that the isotope fractions of the enriched Si are determined; the usual way to measure them is by gas mass spectrometry of  $\text{SiF}_4$ . An analysis carried out at the University of Warsaw evidenced that the solutions used to convert the approximately 45 mg crystal samples into the  $\text{SiF}_4$  gas were contaminated by more than  $7 \mu\text{g}$  of natural Si. This contamination required a correction of about  $0.6 \times 10^{-6}M$ . The isotope fractions were measured also at the Institute of Mineral Resources of the Chinese Academy of Science still by gas mass spectrometry, but using a different preparation of the  $\text{SiF}_4$  gas based on fluorination by

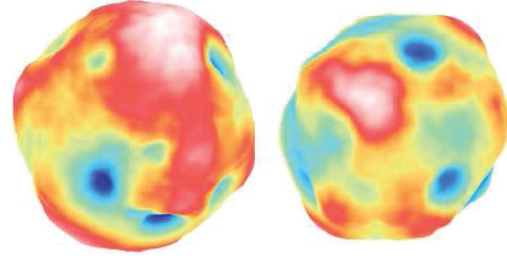


FIG. 3 (color). Diameter topographies of the silicon spheres. The rainbow colors range from  $-63$  nm (blue) to  $37$  nm (red). Peak-to-valley distances are  $97$  nm (AVO28-S5, left) and  $89$  nm (AVO28-S8, right).

$\text{BrF}_5$ . Also in this case the contamination by natural Si proved to be a problem. Furthermore, the extremely high isotopic enrichment proved to be a big challenge; ion current ratios more than 5 orders of magnitude larger than the unity had to be measured.

To overcome these difficulties, a new concept has been developed [11,12]. It is based on isotope dilution mass spectrometry (IDMS) combined with multicollector inductively coupled plasma mass spectrometry—with samples being dissolved in aqueous NaOH. The novelty is that only the  $^{29}\text{Si}^+$  and  $^{30}\text{Si}^+$  currents were measured; to recover the missed  $^{28}\text{Si}$  fraction, the samples were blended with a spike highly enriched with  $^{30}\text{Si}$ . The  $^{30}\text{Si}^+$  and  $^{29}\text{Si}^+$  currents were measured for the sample, spike, and blend; the  $^{28}\text{Si}^+$  current was measured only for the spike. The  $^{28}\text{Si}$  fraction of the sample was obtained by data analysis. Calibration was carried out online by mixtures of natural Si and two crystals enriched with the  $^{29}\text{Si}$  and  $^{30}\text{Si}$  isotopes. Natural Si contamination, memory effects, and offsets were monitored and corrected online by having the NaOH solutions remeasured before each sample, spike, blend, or mixture. The isotopic composition of the  $^{28}\text{Si}$  crystal was determined also at the Institute for Physics of Microstructures of the Russian Academy of Sciences by a secondary ion mass spectrometer (SIMS) using a time-of-flight mass analyzer.

Figure 4 shows the measured  $^{29}\text{Si}$  and  $^{30}\text{Si}$  amount fractions. The highest enrichments are observed by IDMS and SIMS. Continuously adding natural Si to a material having the isotopic composition determined by IDMS, the  $^{29}\text{Si}$  and  $^{30}\text{Si}$  fractions will move along the black line and also pass quite near to the other measurement results. Under this assumption the isotopic compositions determined by IDMS and gas mass spectrometry are consistent with each other. The IDMS data are the most accurate and have been considered only; the relevant molar mass values are given in Table III.

*$N_A$  determination.*—The measured values of the quantities necessary to determine  $N_A$  are summarized in Table III. The  $N_A$  determinations based on two spheres differ only by  $3(3) \times 10^{-8}N_A$ , thus confirming the crystal homogeneity. By averaging these values, we obtain

TABLE III.  $N_A$  determination. Lattice parameter, volume, and density are measured at  $20.0^\circ\text{C}$  and  $0$  Pa.

Quantity	Unit	AVO28-S5	AVO28-S8
$a$	pm	543.099 6240(19)	543.099 6185(20)
$m$	g	1000.087 560(15)	1000.064 543(15)
$V$	$\text{cm}^3$	431.059 059(13)	431.049 110(10)
$\rho$	$\text{kg}/\text{m}^3$	2320.070 855(76)	2320.071 007(63)
$M$	$\text{g}/\text{mol}$	27.976 970 26(22)	27.976 970 29(23)
$N_A$	$10^{23} \text{mol}^{-1}$	6.022 140 91(21)	6.022 140 71(18)



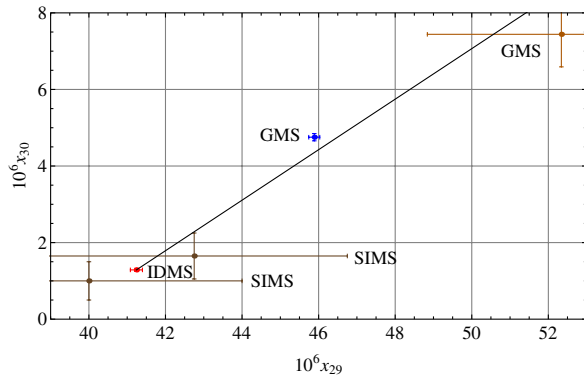


FIG. 4 (color online). Measured isotope amount fractions  $x_{29}$  and  $x_{30}$  of the  $^{28}\text{Si}$  boule as determined by gas mass spectrometry (GMS), secondary ion mass spectrometry (SIMS), and isotope dilution mass spectrometry (IDMS). The solid line indicates the composition locus of fictional samples obtained by adding natural silicon to the enriched silicon measured by IDMS. The bars give the standard uncertainties.

$$N_A = 6.022\,140\,78(18) \times 10^{23} \text{ mol}^{-1}, \quad (1)$$

with  $3.0 \times 10^{-8}$  relative uncertainty. The main contributions to the uncertainty budget are given in Table IV.

**Conclusions.**—For the first time accurate  $h$  values derived from different experiments can be compared. This comparison is a test of the consistency of atomic physics. A parallel experiment, having the purpose of measuring  $N_A h$  by absolute nuclear spectroscopy, is aiming at extending this test to nuclear physics [13]. Figure 5 shows our result compared with those of the two most accurate measurements so far carried out: The watt-balance experiments of the National Institute of Standards and Technology (NIST—U.S.) [2] and the National Physical Laboratory (NPL—U.K.) [14]. The values of the Planck constant measured by these experiments were converted into the corresponding  $N_A$  values by  $N_A h = 3.990\,312\,682\,1(57) \times 10^{-10} \text{ J s/mol}$  [15].

Our result leads to more consistent values for the fundamental physical constants. It is also a step towards demonstrating a successful *mise en pratique* of a kilogram definition based on a fixed  $N_A$  or  $h$  value. The agreement between the different realizations is not yet as good as it is

TABLE IV. Uncertainty budget of the  $N_A$  determination.

Quantity	Relative Uncertainty ( $10^{-9}$ )	Contribution (%)
Molar Mass	6	4
Sphere Mass	3	1
Surface	15	24
Sphere Volume	23	57
Lattice Parameter	11	13
Crystal Perfection	3	1

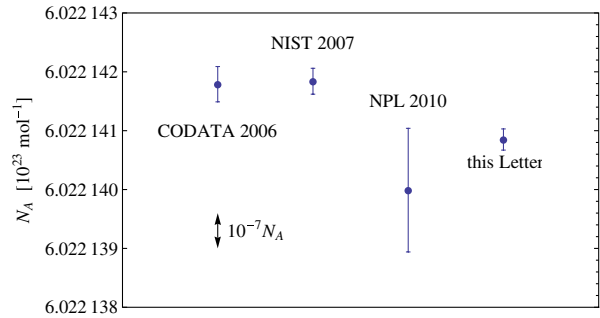


FIG. 5 (color online). Avogadro constant determinations. Comparison between the most accurate values at present available. The bars give the standard uncertainty.

required to retire the Pt-Ir kilogram prototype, but—considering the capabilities already developed and the envisaged improvements in the surface characterization and the volume and lattice parameter measurements—it seems to be realistic that the targeted uncertainty may be achieved in the foreseeable future [16].

We thank A.K. Kaliteevski and his colleagues at the Central Design Bureau of Machine Building and the Institute of Chemistry of High-Purity Substances for their dedication and the delivery of the enriched material, our directors for their advice and financial support, and our colleagues for their daily work. This research received funds from the European Community’s 7th Framework Programme ERA-NET Plus (Grant No. 217257) and the International Science and Technology Center (Grant No. 2630).

- [1] I. M. Mills *et al.*, *Metrologia* **43**, 227 (2006).
- [2] R. L. Steiner *et al.*, *IEEE Trans. Instrum. Meas.* **56**, 592 (2007).
- [3] P. Becker *et al.*, *Meas. Sci. Technol.* **20**, 092002 (2009).
- [4] P. J. Mohr and B. N. Taylor, *Rev. Mod. Phys.* **72**, 351 (2000).
- [5] P. Becker *et al.*, *Meas. Sci. Technol.* **17**, 1854 (2006).
- [6] P. Becker and D. Windisch, *Phys. Status Solidi A* **118**, 379 (1990).
- [7] M. P. Seah *et al.*, *Surf. Interface Anal.* **36**, 1269 (2004).
- [8] S. Mizushima, *Metrologia* **41**, 137 (2004).
- [9] I. Busch *et al.*, *IEEE Trans. Instrum. Meas.* **58**, 891 (2009).
- [10] R. A. Nicolaus and K. Fujii, *Meas. Sci. Technol.* **17**, 2527 (2006).
- [11] O. Rienitz *et al.*, *Int. J. Mass Spectrom.* **289**, 47 (2010).
- [12] G. Mana and O. Rienitz, *Int. J. Mass Spectrom.* **291**, 55 (2010).
- [13] S. Rainville *et al.*, *Nature (London)* **438**, 1096 (2005).
- [14] I. A. Robinson and B. P. Kibble, *Metrologia* **44**, 427 (2007); (Private communication).
- [15] P. J. Mohr, B. N. Taylor, and D. B. Newell, *Rev. Mod. Phys.* **80**, 633 (2008).
- [16] M. Glaeser *et al.*, *Metrologia* **47**, 419 (2010).